iScience

CellPress
OPEN ACCESS

Article

Moderate-intensity aerobic exercise training improves CD8$^+$ tumor-infiltrating lymphocytes effector function by reducing mitochondrial loss

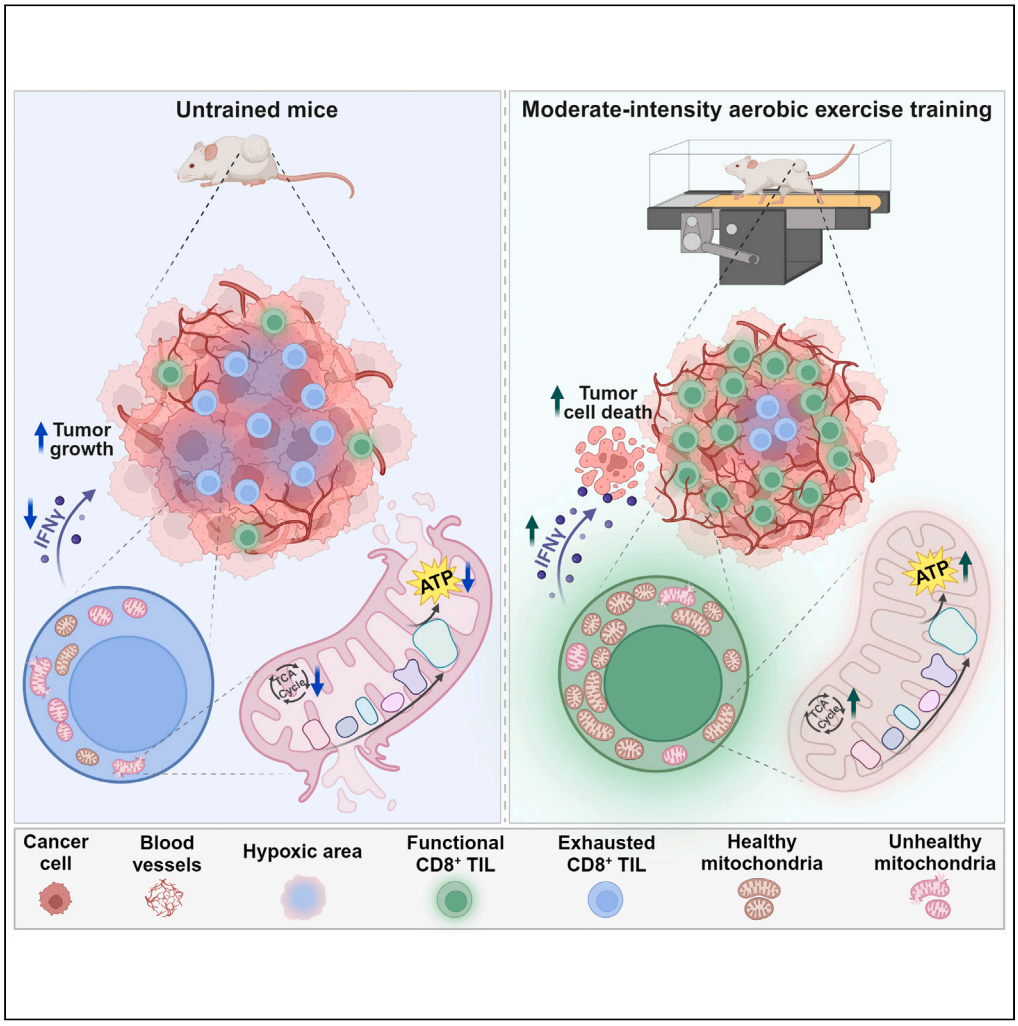

Vanessa Azevedo Voltarelli, Mariane Tami Amano, Gabriel Cardial Tobias, ..., James Edward Turner, Patricia Chakur Brum, Anamaria Aranha Camargo

vvoltare@bidmc.harvard.edu

Highlights

Exercise training reduces tumor growth and improves survival in colorectal cancer

Trained mice present tumors with less hypoxia and higher CD8$^+$ T cells infiltration

The production of IFNγ by CD8$^+$ TIL is increased in exercise-trained mice

CD8$^+$ TIL from trained mice show higher mitochondrial density and function

Voltarelli et al., iScience *27*, 110121
June 21, 2024
https://doi.org/10.1016/j.isci.2024.110121

iScience

CellPress
OPEN ACCESS

Article

Moderate-intensity aerobic exercise training improves CD8$^+$ tumor-infiltrating lymphocytes effector function by reducing mitochondrial loss

Vanessa Azevedo Voltarelli,[1,2,3,13,*] Mariane Tami Amano,[1] Gabriel Cardial Tobias,[2,4] Gabriela Silva Borges,[2] Ailma Oliveira da Paixão,[2] Marcelo Gomes Pereira,[2,5] Niels Olsen Saraiva Câmara,[6] Waldir Caldeira,[7] Alberto Freitas Ribeiro,[7] Leo Edmond Otterbein,[3] Carlos Eduardo Negrão,[2,8] James Edward Turner,[9,10] Patricia Chakur Brum,[2,11,12] and Anamaria Aranha Camargo[1,12]

SUMMARY

Aerobic exercise training (AET) has emerged as a strategy to reduce cancer mortality, however, the mechanisms explaining AET on tumor development remain unclear. Tumors escape immune detection by generating immunosuppressive microenvironments and impaired T cell function, which is associated with T cell mitochondrial loss. AET improves mitochondrial content and function, thus we tested whether AET would modulate mitochondrial metabolism in tumor-infiltrating lymphocytes (TIL). Balb/c mice were subjected to a treadmill AET protocol prior to CT26 colon carcinoma cells injection and until tumor harvest. Tissue hypoxia, TIL infiltration and effector function, and mitochondrial content, morphology and function were evaluated. AET reduced tumor growth, improved survival, and decreased tumor hypoxia. An increased CD8$^+$ TIL infiltration, IFN-γ and ATP production promoted by AET was correlated with reduced mitochondrial loss in these cells. Collectively, AET decreases tumor growth partially by increasing CD8$^+$ TIL effector function through an improvement in their mitochondrial content and function.

INTRODUCTION

In 2018, the national expenditure for cancer care in the United States was estimated at $150.8 billion. Costs are likely to increase due to increase in lifespan and the adoption of new and more expensive treatments, such as checkpoint inhibitor immunotherapy.[1,2] Therefore, a better understanding of factors and environmental conditions that can prevent or decrease cancer incidence and mortality would be of great value. Aerobic exercise training (AET) reduces the incidence and mortality of several cancer types.[3–10] In 2016, Moore and collaborators showed that among 1.44 million adults from USA and Europe, high levels of leisure-time physical activity were positively correlated with a significant reduction in the incidence of 13 types of cancer.[11] Furthermore, the World Cancer Research Fund (WCRF) points out that moderate physical activity (such as brisk walking) as well as vigorous physical activity (including running, fast cycling, and aerobics) decreases the risk of colon, womb, and post-menopausal breast cancer.[12] Previous clinical findings also indicated that cancer patients with reduced aerobic capacity present a poorer prognosis of the disease.[13–16]

While epidemiological studies indicate that high levels of physical activity in general reduce the risk of cancer development, it is likely that the anti-cancer mechanisms are most robustly stimulated by structured and long-term moderate-to-vigorous intensity AET.[17] However, these molecular mechanisms underlying the benefits of AET on cancer incidence and mortality are still poorly understood. There is an increasing number of studies addressing this question that provide new insights into potential mechanisms of action by which exercise reduces tumor growth and progression, including the modulation of systemic and intratumoral immunity.[18–20] Tumors escape initial immune detection by generating an immunosuppressive intratumoral microenvironment which limits immune cell infiltration, activation, and effector function.

[1]Molecular Oncology Center, Sírio-Libanês Hospital, São Paulo, SP, Brazil
[2]School of Physical Education and Sport, University of São Paulo, São Paulo, SP, Brazil
[3]Department of Surgery, Beth Israel Deaconess Medical Center, Harvard Medical School, Boston, MA, USA
[4]Department of Pediatrics, Weill Cornell Medical College, New York, NY, USA
[5]Leeds School of Biomedical Sciences, Faculty of Biological Sciences, University of Leeds, Leeds, UK
[6]Department of Immunology, Institute of Biomedical Sciences, University of São Paulo, São Paulo, SP, Brazil
[7]Department of Genetics and Evolutionary Biology, University of São Paulo, São Paulo, SP, Brazil
[8]Heart Institute, Faculty of Medicine, University of São Paulo, São Paulo, SP, Brazil
[9]Department for Health, University of Bath, Bath, UK
[10]School of Sport, Exercise and Rehabilitation Sciences, University of Birmingham, Birmingham, UK
[11]Department of Physiology & Biophysics, Institute of Biomedical Sciences, University of São Paulo, São Paulo, SP, Brazil
[12]These authors contributed equally
[13]Lead contact
*Correspondence: vvoltare@bidmc.harvard.edu
https://doi.org/10.1016/j.isci.2024.110121

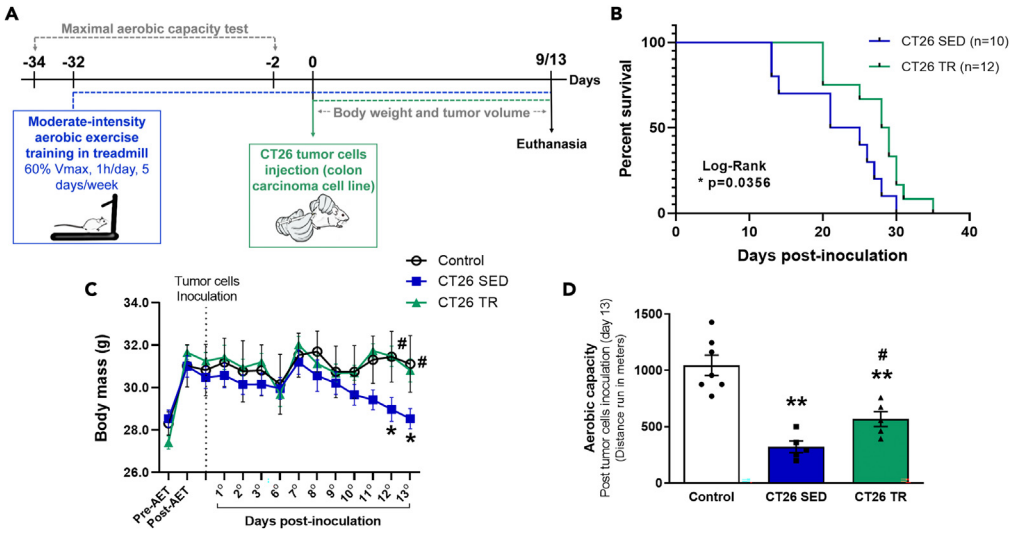

Figure 1. Moderate-intensity aerobic exercise training increases survival and aerobic capacity in mice with colorectal cancer

(A) Study experimental design, (B) survival rates, (C) body mass changes post-tumor cell inoculation, and (D) aerobic capacity represented as distance run in meters during an exhaustion test on day 13 after tumor cell inoculation, comparing sedentary animals (control), sedentary tumor-bearing mice (CT26 SED), and trained tumor-bearing mice (CT26 TR). Data represent mean ± SEM. Comparison of survival curves by log rank (Mantel-Cox) test (*p = 0.0356). Repeated measures ANOVA, and one-way ANOVA, followed by Duncan's post hoc. *$p < 0.05$, **$p < 0.01$ vs. control, and #$p < 0.05$ vs. CT26 SED.

Recent studies have shown that exercise can modulate immune cell mobilization and anti-tumor immunity.[21] For example, Rundqvist and collaborators using a mouse model of breast cancer showed that voluntary exercise-mediated reduction in tumor growth is dependent on cytotoxic $CD8^+$ T cell infiltration, and that skeletal muscle metabolites released during high intensity exercise into plasma enhances $CD8^+$ T cell effector function.[19] Others have also demonstrated that exercise enhances $CD8^+$ T cell infiltration and effector function and improves responses to checkpoint inhibitors immunotherapy.[22]

Mitochondrial dynamics and metabolism have been identified as key modulators of tumor-infiltrating lymphocytes (TIL) fate and effector function.[23–25] Impaired TIL effector function has been associated with a persistent loss of mitochondrial content and function, which is directly associated with a decrease in interferon-gamma (IFN-γ) production. Additionally, impaired TIL effector function was shown to be tumor microenvironment (TME) specific, and largely independent of PD-1 blockade or regulatory T cell suppression.[24] Also, mitochondrial dysfunction in $CD8^+$ TIL has been shown to reinforce phenotypic and epigenetic reprograming for T exhaustion.[25]

AET improves aerobic fitness and metabolism, which occurs primarily through significant increases in mitochondria number, volume, and function in different body tissues.[26] Therefore, in the present study we tested the hypothesis that AET would modulate TIL mitochondrial content, function, and morphology, thereby preventing or mitigating impairment of their effector function. The key findings of our study are that moderate-intensity AET improves survival and morbidity while reducing tumor growth in the CT26 animal model of colorectal cancer. These outcomes were associated with an increase in both the number and effector function of $CD8^+$ TILs. We also found that AET prevents the loss of $CD8^+$ TIL mitochondrial density and function, and that this is associated with an improved effector/cytotoxic $CD8^+$ TIL function.

RESULTS

Aerobic exercise training increases survival and reduces morbidity in a colorectal cancer mice model

The experimental design of the study is shown in Figure 1A. Moderate-intensity AET performed prior to tumor cell inoculation and continued during tumor development improved overall survival in tumor-bearing trained mice (CT26 TR) compared to tumor-bearing sedentary mice (CT26 SED) (Figure 1B). CT26 TR mice also showed a less pronounced body weight loss and improved aerobic capacity at day 13 after tumor cell inoculation compared to CT26 SED group (46% vs. 69% drop in total distance, $p < 0.01$), (Figures 1C and 1D). CT26 TR mice exhibited a decrease in epididymal fat mass but no significant difference in tibialis, soleus, and gastrocnemius muscles masses compared to CT26 SED mice (Figures S1A–S1D). These data indicate that AET attenuates cancer-related morbidity while improving survival.

Aerobic exercise training reduces tumor latency, growth and hypoxic core, and increases immune cell tumor infiltration

CT26 TR mice showed a delay in tumor latency compared to CT26 SED group as assessed by the detection of palpable tumors (Figure 2A). Also, moderate-intensity AET significantly decreased tumor growth measured over 13 days post-inoculation (Figures 2A and 2B). The greatest difference in tumor growth and *ex vivo* mass was observed at day 9 (Figures 2C–2E) and thus, all further analyses were performed on tumors harvested on day 9 post-inoculation, since we considered this time point as the one with maximum effect of AET on tumor growth.

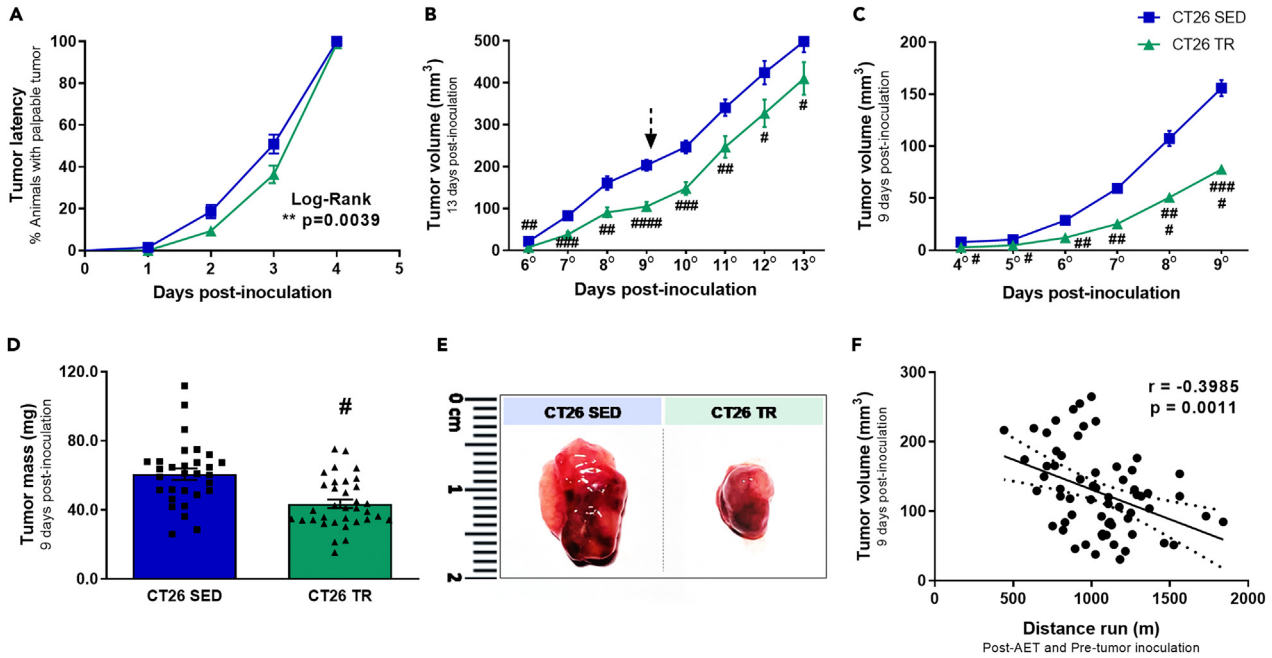

Figure 2. Moderate-intensity aerobic exercise training decreases CT26 tumor growth in mice with colorectal

(A) Tumor latency, (B) tumor volume measured for 13 days following CT26 cells inoculation; arrow indicates the time with the largest statistical difference between groups (9 days), (C) tumor volume measured up to day 9 after tumor cell inoculation, (D) *ex vivo* tumor mass at day 9, (E) representative images of *ex vivo* solid tumors at day 9, and (F) correlation between aerobic capacity evaluated after AET and before CT26 inoculation and tumor volume measured at day 9 comparing sedentary tumor-bearing mice (CT26 SED) and trained tumor-bearing mice (CT26 TR). Data represent mean ± SEM. Tumor latency curves by log rank (Mantel-Cox) test (**$p = 0.0039$). Unpaired Student's t test. #$p < 0.05$, ##$p < 0.01$, ###$p < 0.001$, and ####$p < 0.0001$ vs. CT26 SED.

Interestingly, we observed a significant negative correlation between aerobic capacity evaluated before tumor cell inoculation and tumor volume measured at day 9, indicating that improved aerobic capacity has a quantitative effect on tumor growth. (Figure 2F). In addition to the effects on tumor growth, AET significantly reduced the percentage of hypoxic areas within the TME of CT26 TR mice compared to CT26 SED mice (Figures 3A–3C), which was accompanied by an increase in the number of infiltrating immune cells (Figures 3D and 3E).

Aerobic exercise training modulates the composition and function of TILs

In parallel with an increased number of immune cells infiltrating the TME, we observed that AET specifically increases the total number of tumor-infiltrating T cells when compared to CT26 SED (Figures 4A–4D). When distinguishing TIL by their subpopulations, we observed that the population of $CD4^+$ T cells did not statistically differ among the CT26 SED and CT26 TR groups (Figure 4E), while the number of regulatory T cells (Treg) showed a significant decrease in CT26 TR in comparison to CT26 SED mice (Figure 4F). The decreased percentage of Treg cells in tumors of trained mice supports the significant increase in the population of $CD8^+$ T cells in the CT26 TR group, which was accompanied by a significant increase in the percentage of activated $CD8^+$ T cells when compared to CT26 SED mice (Figures 5A and 5B). In accordance, CT26 TR mice showed a higher population of $CD8^+$ T cells in the draining lymph nodes (dLN) compared to CT26 SED mice (Figure S2C).

$CD8^+$ TIL function was also evaluated by measuring IFNγ, since this cytokine is critical for T cell effector function against tumor cells.[27] AET significantly increased the percentage of $IFN\gamma^+$ $CD8^+$ T cells in tumors of CT26 TR compared to CT26 SED (Figures 5C and 5D), indicating that $CD8^+$ TILs from CT26 TR mice are more capable of producing IFNγ and potentially killing tumor cells. However, there were no statistically significant differences between groups for $CD8^+$ TIL populations positively expressing the checkpoint receptor $PD\text{-}1^+$ (Figure 5E), indicating that this mechanism is not associated with reduced tumor growth and with increased infiltration of effector T cells induced by AET.

Aerobic exercise training prevents loss of $CD8^+$ TIL mitochondrial content and function, which is associated with increased IFNγ production

It has been shown that morphological changes in mitochondria, controlled by the balance between mitochondrial fusion and fission, are a primary signal that shapes metabolic reprogramming during T cell quiescence and activation.[23,25] Therefore, electron microscopy images of $CD8^+$ TIL isolated from CT26 SED and CT26 TR mice were analyzed but showed no significant differences between groups for the different mitochondrial morphology parameters evaluated (mitochondrial area, elongation, and circularity). The only significant difference observed was that $CD8^+$ TILs from CT26 TR exhibited an increased number of mitochondria when compared to TILs from CT26 SED mice

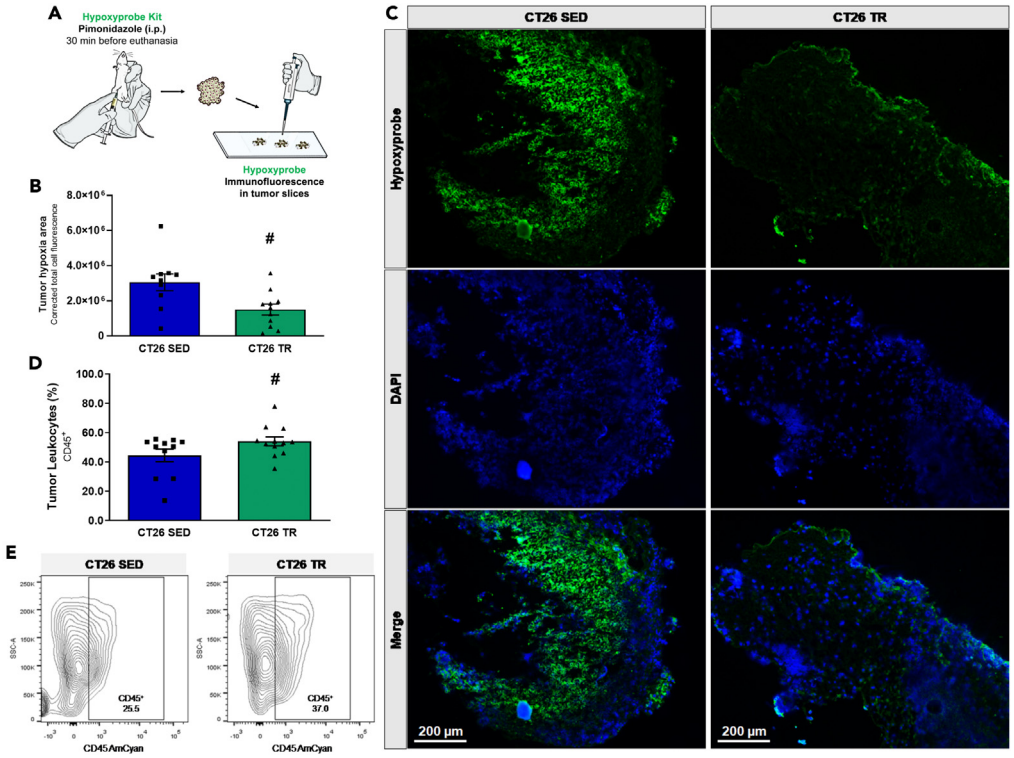

Figure 3. Aerobic exercise training decreases tumor hypoxia while increasing total tumor-infiltrating immune cells

(A) Experimental protocol, (B) tumor hypoxic area quantitatively measured by fluorescence, (C) immunohistological images (100x) of tumor sections stained with DAPI (nuclear), a pimonidazole primary antibody (Hypoxyprobe), followed by a FITC-secondary antibody incubation, and (D and E) total tumor-infiltrating leukocytes percentage ($CD45^+$) analyzed by flow cytometry comparing sedentary tumor-bearing mice (CT26 SED) and trained tumor-bearing mice (CT26 TR) at day 9 post-tumor cell inoculation. Data represent mean ± SEM. Unpaired Student's t test. #$p < 0.05$ vs. CT26 SED.

(Figures 6A–6E). Corroborating these data, CT26 TR $CD8^+$ TIL exhibited a significant increase in mitochondrial density evaluated by MitoTracker Green when compared to TILs from CT26 SED mice (Figure 6F). Interestingly, when $CD8^+$ TIL mitochondrial densities of tumor-bearing mice were compared to the mitochondrial density of T cells isolated from inguinal lymph nodes of healthy sedentary control mice, we observed that both CT26 SED and CT26 TR lymphocytes infiltrating the TME lost a significant amount of mitochondrial content. Even though AET was unable to bring TILs mitochondrial content to control levels, $CD8^+$ TIL loss of mitochondrial density in CT26 TR mice was partially prevented when compared to CT26 SED (Figure 6G). We also showed that the total TILs from CT26 TR exhibit an increase in protein expression of mitochondrial complex III when compared to CT26 SED mice, with no significant changes in mitochondrial complexes I, II, and IV expressions (Figure S2E). However, the total TILs protein expression of dynamin-like GTPase Mitofusin 1 (Mfn1), essential for mitochondrial fusion,[28] was not different between the groups (Figure S3A). In addition, no significant differences were observed in the gene expression of PINK1, PARK2, ULK1, BNIP3, ATG5, ATG7, and LC3B, markers of autophagy/mitophagy,[29,30] in the solid tumors of CT26 TR compared to CT26 SED mice (Figures S3B–S3H).

As can be seen in Figures 6H and 6I, the partial increase in $CD8^+$ TILs mitochondrial density by AET was associated with an increased number of healthy/functional mitochondria in these cells, since $CD8^+$ TIL from CT26 TR showed a higher mitochondrial membrane potential ($\Delta\Psi M$), represented by the red/green fluorescence ratio (healthy/unhealthy mitochondria), when compared to TIL from CT26 SED mice. In addition, AET significantly increased the ATP production of the total tumor-infiltrating immune cells compared to sedentary controls, suggesting that AET not only induces an increase in mitochondrial content, but also improves their oxidative phosphorylation (OXPHOS) function (Figure 6J). Indeed, an *in-silico* analysis of a public microarray dataset (Geo Dataset GSE68072,[31]) comparing peripheral blood leukocytes in young endurance athletes (outside the competition period) to non-athletes at rest, showed that the leukocytes of athletes present an increase in expression of OXPHOS genes compared to non-athletes (Figure S2D).

To determine if there is a direct and positive association between mitochondrial content/function and the T cell effector function, leukocytes were isolated from draining lymph nodes (inguinal) of CT26 SED and CT26 TR animals. The cells were treated with oligomycin (a mitochondrial ATP synthase inhibitor), and FCCP (a mitochondrial uncoupler, widely used for assessing maximal oxygen consumption by mitochondria). We observed that $CD8^+$ T cells isolated from CT26 TR mice showed an increase in IFNγ production compared to CT26 SED mice when maximal mitochondrial function was induced with FCCP. No significant differences were observed between the groups for the baseline and the oligomycin conditions (Figures 6K and 6L). These data suggest that the enhanced oxidative metabolism promoted by

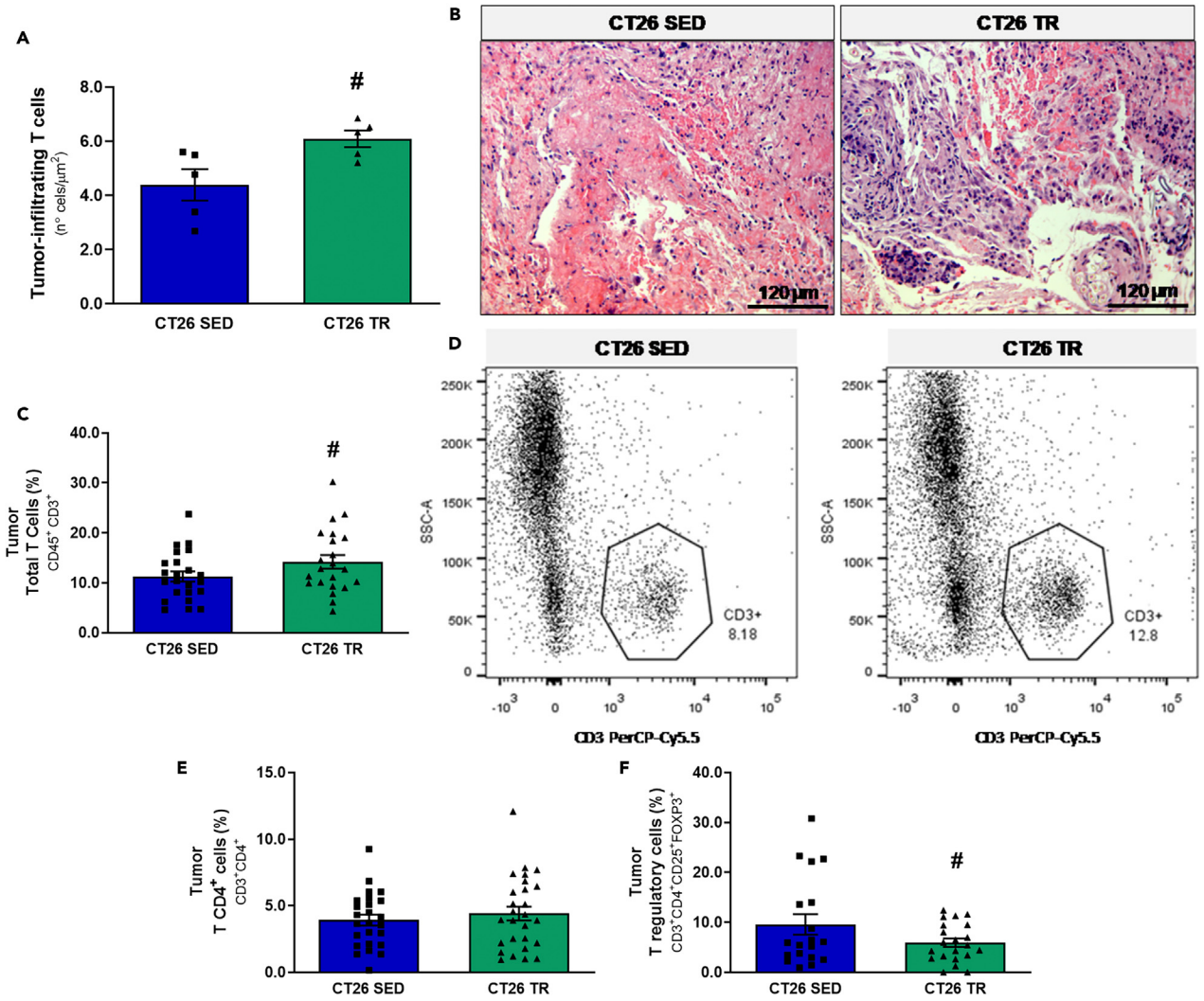

Figure 4. Tumor-infiltrating T cell populations are modulated by aerobic exercise training

(A and B) Tumor-infiltrating T cells evaluated in tumor histological sections stained with hematoxylin-eosin (200x), (C and D) total TILs ($CD3^+$) evaluated by flow cytometry, (E) total tumor-infiltrating $CD4^+$ T cells, and (F) regulatory T cells (Treg), comparing sedentary tumor-bearing mice (CT26 SED) and trained tumor-bearing mice (CT26 TR). Data represent mean ± SEM. Unpaired Student's t test. #$p < 0.05$ vs. CT26 SED.

AET can lead to increased effector function of $CD8^+$ T cells in tumor-bearing mice, which may partially contribute to the observed decreased tumor growth in CT26 TR compared to CT26 SED mice.

DISCUSSION

The principal findings of the present study were that AET inhibited tumor growth and limited the hypoxic area of the TME, which correlated with an increase in both the number and effector function of $CD8^+$ TILs. In addition, in sedentary mice, $CD8^+$ TILs exhibited reduced mitochondrial content and function, which was prevented in part by AET. Finally, $CD8^+$ T cells from AET mice exhibited elevated IFNγ, which was accompanied by induction of maximal mitochondrial function, supporting a cause-and-effect relationship between improved $CD8^+$ T cell mitochondrial bioenergetics and effector functionality.

The beneficial effects of AET in reducing cancer incidence and the tumor growth have been extensively shown.[8,20,32–34] Here, we corroborate those findings using a colorectal cancer animal model, in which a moderate-intensity AET protocol performed before and after tumor cells inoculation significantly decreased tumor growth while increasing the survival rate and reducing morbidity. In support, Lakoski and collaborators showed in 2015 that lung and colon cancer patients with greater physical capacity exhibited longer survival rates compared to patients with less physical capacity.[35] It had also been demonstrated that colon cancer patients present a reduction, greater than 20%, in their maximum oxygen consumption ($VO_{2\ max}$) compared to their healthy peers, which is followed by reduced lean mass measured in their legs.[14] Considering that, AET is known to attenuate the loss of body and skeletal muscle masses, which is usually triggered by pro-cachectic types of

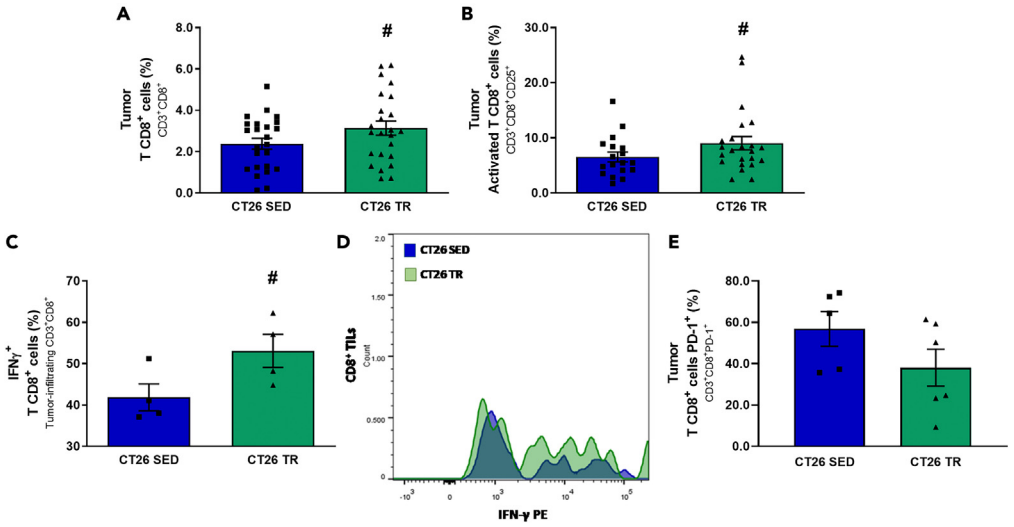

Figure 5. Aerobic exercise training increases the number and function of CD8$^+$ tumor-infiltrating T cells

(A and B) Total and activated tumor-infiltrating CD8$^+$ T cells, and the populations of (C and D) IFN-γ$^+$ and (E) PD-1$^+$ CD8$^+$ TILs, comparing sedentary tumor-bearing mice (CT26 SED) and trained tumor-bearing mice (CT26 TR). Data represent mean ± SEM. Unpaired Student's t test. #$p < 0.05$ vs. CT26 SED.

cancer, such as colon cancer.[36,37] Encouragingly, our data show that AET can prevent the loss of body mass, associated with an attenuated loss of aerobic capacity that was induced by cancer progression. It is important to highlight, however, that a recent study has shown that exercise worsened survival in colorectal tumor-bearing mice when performed in association with chemotherapy in late stages of cachexia.[38]

Our findings can be partially explained by the effects of AET on the TME at a cellular level. We here propose, based on previous studies in the literature,[32,39,40] that AET increases tumor perfusion through an improved functional angiogenesis, which facilitate the infiltration of immune cells in the TME, as seen in Figures 3D and 3E. The increased number of functional blood vessels irrigating the TME induced by the AET will further reduce the TME hypoxic areas, as shown in Figures 3B and 3C. The reduced area of hypoxia, in turn, improves the effector function of CD8$^+$ T cells by preventing their loss of mitochondrial content and activity. In fact, it has been previously shown that dysfunctional vascularization and its consequent hypoxic areas can lead to metabolic exhaustion of immune cells infiltrating the TME.[39–41]

In support, our data show that AET increases the number of activated CD8$^+$ TIL populations, which exhibit increased IFNγ production. The improved CD8$^+$ TIL function induced by AET may also be partially related to the reduced population of Treg cells in the TME, since these are known to suppress the cytotoxic function of immune cells.[42]

Improvements in metabolic control is another important factor to be considered as being partially responsible for increased CD8$^+$ TIL effector function in trained mice. Since activated T cells depend on aerobic glycolysis to produce ATP,[43] the mitochondria function plays an essential role on T cells, besides being historically neglected in the literature. However, mitochondria cannot just be seen as an ATP source, considering that these organelles are also involved in calcium homeostasis, lipid synthesis, apoptosis, signaling, and cell cycle progression.[44] In fact, mitochondrial metabolism has been shown to play a key role in the differentiation and in fate of T cells.[25,45] Although there is evidence demonstrating that an increased OXPHOS reduces IFNγ secretion by T cells,[46] it has recently been shown that, during their first hours of activation, T cells dramatically increase mitochondrial mass, as well as mitochondrial DNA levels,[46] and that this mitochondrial biogenesis induction is indispensable for them to escape quiescence.[47] This evidence corroborates our results that show a positive and direct effect of the maximal mitochondrial function on IFNγ production by CD8$^+$ T cells, associated with an attenuated loss of mitochondrial density in TIL by the AET. A significant increase in ATP production and in the mitochondrial complex III expression in tumor-infiltrating leukocytes was also promoted by AET (Figure S2). It is important to highlight that complex III is an important reactive oxygen species (ROS) source in mitochondria, and that mitochondrial ROS production is important for T cell activation.[43,48] Moreover, T cells that do not express the complex III subunit Uqcrfs1, necessary to produce mitochondrial ROS, are not able to produce IL-2, a cytokine that is essential for maturation and proliferation. Besides being a well-accepted index of mitochondrial health and functionality,[23,25] CD8$^+$ TIL mitochondria morphology was not changed by AET, even though a significant increase in the $\Delta\Psi M$ was seen in these cells when compared to the sedentary group. Additionally, the morphology data indicate that the increased mitochondrial number showed in the CD8$^+$ TIL from trained mice cannot be explained by the process of mitochondrial fission.

The discovery of new mechanisms associated with a reduced tumor growth promoted by the AET might support the future development of pharmacological and non-pharmacological therapies for treating cancer. In this regard, it is relevant to highlight that metformin, an approved medication used in patients with diabetes, has been pointed as a potential drug in oncology clinic, since observational studies reported decreased cancer incidence and cancer-related mortality among people taking this medication.[49,50] The mechanisms of action of its anticancer properties are still under investigation, but one strong candidate is the activation of AMP-activated protein kinase (AMPK), an energy sensor that regulates cellular and mitochondrial metabolism and which is well known to be highly activated by aerobic exercise.[51]

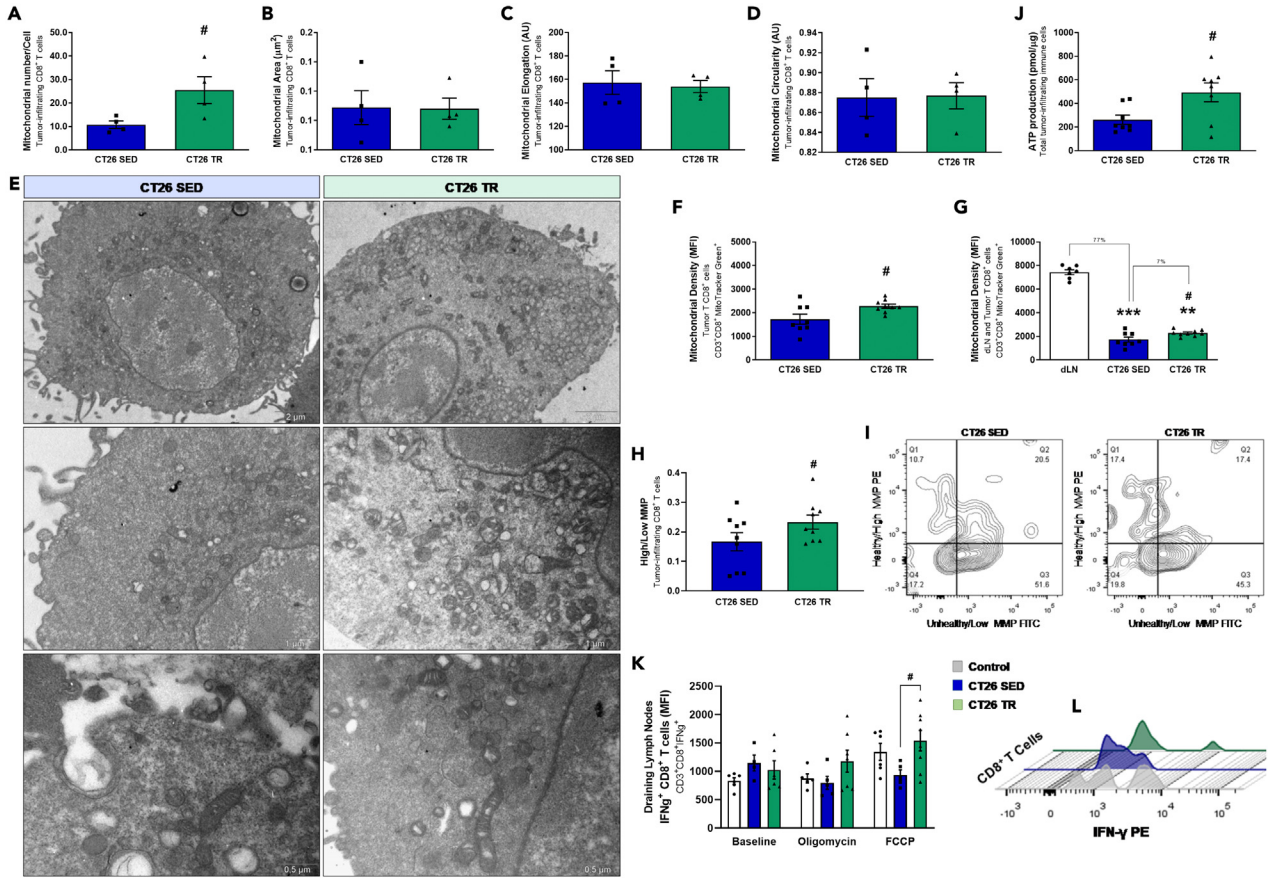

Figure 6. Increased IFNγ production in CD8$^+$ TILs promoted by aerobic exercise training is associated with improved mitochondrial density and function

(A) Mitochondrial number per cell, (B–D) area, elongation, and circularity of CD8$^+$ TILs isolated using magnetic beads, and (E) representative transmission electron microscopy images, (F) CD8$^+$ TILs mitochondrial density evaluated by the MitoTracker Green fluorescent probe, (G) and compared to the mitochondrial density of inguinal lymph node CD8$^+$ T cells harvested from healthy sedentary controls (white bars), (H and I) the ratio between CD8$^+$ TILs with high and low mitochondrial membrane potential (healthy and unhealthy mitochondria, respectively) evaluated by the JC-1 fluorescent probe, and (J) ATP production by total tumor-infiltrating leukocytes comparing sedentary tumor-bearing mice (CT26 SED) and trained tumor-bearing mice (CT26 TR).

(K and L) Production of IFNγ (median fluorescence intensity, MFI) by draining lymph node (dLN) CD8$^+$ T cells under baseline condition, and in response to oligomycin (mitochondrial ATP synthase inhibitor) and FCCP (inducer of maximal oxygen consumption by mitochondria), comparing sedentary animals (control), sedentary tumor-bearing mice (CT26 SED), and trained tumor-bearing mice (CT26 TR). Data represent mean ± SEM. Unpaired Student's t test, and one-way ANOVA, followed by Duncan's post hoc. $^{**}p < 0.01$, $^{***}p < 0.001$ vs. control, and $\#p < 0.05$ vs. CT26 SED.

Accordingly, activators of AMPK, such as AICAR (5-aminoimidazole-4-carboxamide ribonucleoside), are currently some of the most effective exercise mimetics emerging as therapeutic targets.[52,53] Moreover, as muscle-derived myokines that are released during exercise (e.g., IL-6 and IL-15) have been shown to regulate the TME and its infiltrating immune cells,[54,55] future studies are needed to better understand muscle-tumor crosstalk within the context of AET and its potential clinical utility in the treatment of cancer. Therefore, the use of exercise mimetics in oncology, and the formal inclusion of exercise training protocols for cancer patients as adjuvant therapies should be encouraged as more scientific evidence accumulates.

Taken together, we provide evidence that a structured moderate intensity AET, performed before and after tumor establishment, increases survival rate and decreases morbidity and tumor growth through the modulation of CD8$^+$ TIL effector function and their mitochondrial content and function in a mouse model of colorectal cancer. Altogether, we provide new insights on the molecular and immunological mechanisms whereby AET controls tumor growth and progression.

Limitations of the study

While we presented evidence of a potential new mechanism by which AET may modulate the metabolism and function of CD8$^+$ TILs, it's important to acknowledge several limitations in our study. Our hypothesis was tested only in a heterotopic colorectal cancer model, implying that the reported findings might not generalize across other cancer types or even orthotopic colorectal models subjected to AET. Moreover,

based on the data presented, we cannot definitively conclude that the observed effects of AET on $CD8^+$ TILs mitochondrial density and effector function are entirely direct, as they may be influenced by other TME components also modulated by exercise, such as angiogenesis, innervation, tumor cell metabolism, and various immune cell types.[56]

Another limitation lies in our analysis of the isolated mitochondrial morphology of $CD8^+$ TILs, as the T cell purification process from digested tumors could potentially induce significant changes in mitochondrial dynamics and function. Ideally, the evaluation of gold-labeled $CD8^+$ T cell mitochondria content in tumors fixed for electron microscopy immediately after harvest would provide more accurate insights.

Therefore, these limitations highlight the need for further investigation into the effects of AET on $CD8^+$ TILs mitochondrial metabolism in the field of cancer research. Additional studies are needed to corroborate and supplement our findings, as well as those of other studies in the literature of cancer and exercise.

STAR★METHODS

Detailed methods are provided in the online version of this paper and include the following:

- KEY RESOURCES TABLE
- RESOURCE AVAILABILITY
  - Lead contact
  - Materials availability
  - Data and code availability
- EXPERIMENTAL MODEL AND STUDY PARTICIPANT DETAILS
  - Animal model
  - Running capacity test and aerobic exercise protocol
  - CT26 colon carcinoma cell line
- METHOD DETAILS
  - Tumor histology
  - Tumor digestion
  - Flow cytometry
  - ELISpot (Enzyme-Linked ImmunoSpot)
  - ATP production in total leukocytes
  - Immunoblotting
  - Quantitative real-time PCR
  - Transmission Electron Microscopy (TEM)
  - In-silico analysis of a microarray dataset
- QUANTIFICATION AND STATISTICAL ANALYSIS
  - Statistical analysis

SUPPLEMENTAL INFORMATION

Supplemental information can be found online at https://doi.org/10.1016/j.isci.2024.110121.

ACKNOWLEDGMENTS

The authors want to thank Fundação de Amparo à Pesquisa do Estado de São Paulo for the financial support (FAPESP, 2015/22814-5, and 2017/13133-0).

AUTHOR CONTRIBUTIONS

Conceptualization: V.A.V., M.T.A., G.C.T., P.C.B., and A.A.C.; intellectual contribution: V.A.V., M.T.A., G.C.T., J.T., P.C.B., and A.A.C.; methodology and data acquisition: V.A.V., M.T.A., G.S.B., A.O.P., M.G.P., N.O.S.C., W.C., and A.F.R.; formal analysis: V.A.V.; resources: C.E.N., J.T., P.C.B., and A.A.C.; writing—original draft preparation: V.A.V. and L.E.O.; writing—review and editing: V.A.V., M.T.A., G.C.T., L.E.O., J.T., A.A.C., and P.C.B.; supervision: P.C.B. and A.A.C. All authors have read and agreed to the published version of the manuscript.

DECLARATION OF INTERESTS

The authors declare no competing interest.

Received: October 17, 2023
Revised: February 9, 2024
Accepted: May 24, 2024
Published: May 27, 2024

REFERENCES

1. Mariotto, A.B., Robin Yabroff, K., Shao, Y., Feuer, E.J., and Brown, M.L. (2011). Projections of the cost of cancer care in the United States: 2010-2020. J. Natl. Cancer Inst. *103*, 117–128. https://doi.org/10.1093/jnci/djq495.
2. JEMAL, A., VINEIS, P., BRAY, F., TORRE, L., and FORMAN, D. (2019). In THE CANCER ATLAS Third, J.M. Daniel, ed. (American Cancer Society).
3. Michna, L., Wagner, G.C., Lou, Y.R., Xie, J.G., Peng, Q.Y., Lin, Y., Carlson, K., Shih, W.J., Conney, A.H., and Lu, Y.P. (2006). Inhibitory effects of voluntary running wheel exercise on UVB-induced skin carcinogenesis in SKH-1 mice. Carcinogenesis *27*, 2108–2115. https://doi.org/10.1093/carcin/bgl057.
4. Goh, J., Tsai, J., Bammler, T.K., Farin, F.M., Endicott, E., and Ladiges, W.C. (2013). Exercise training in transgenic mice is associated with attenuation of early breast cancer growth in a dose-dependent manner. PLoS One *8*, e80123. https://doi.org/10.1371/journal.pone.0080123.
5. Wolff, G., Balke, J.E., Andras, I.E., Park, M., and Toborek, M. (2014). Exercise modulates redox-sensitive small GTPase activity in the brain microvasculature in a model of brain metastasis formation. PLoS One *9*, e97033–e97038. https://doi.org/10.1371/journal.pone.0097033.
6. Ju, J., Nolan, B., Cheh, M., Bose, M., Lin, Y., Wagner, G.C., and Yang, C.S. (2008). Voluntary exercise inhibits intestinal tumorigenesis in Apc(Min/+) mice and azoxymethane/dextran sulfate sodium-treated mice. BMC Cancer *8*, 316. https://doi.org/10.1186/1471-2407-8-316.
7. Roebuck, B.D., McCaffrey, J., and Baumgartner, K.J. (1990). Protective Effects of Voluntary Exercise during the Postinitiation Phase of Pancreatic Carcinogenesis in the Rat. Cancer Res. *50*, 6811–6816.
8. Hojman, P., Fjelbye, J., Zerahn, B., Christensen, J.F., Dethlefsen, C., Lonkvist, C.K., Brandt, C., Gissel, H., Pedersen, B.K., and Gehl, J. (2014). Voluntary exercise prevents cisplatin-induced muscle wasting during chemotherapy in mice. PLoS One *9*, e109030. https://doi.org/10.1371/journal.pone.0109030.
9. Betof, A.S., Lascola, C.D., Weitzel, D., Landon, C., Scarbrough, P.M., Devi, G.R., Palmer, G., Jones, L.W., and Dewhirst, M.W. (2015). Modulation of murine breast tumor vascularity, hypoxia and chemotherapeutic response by exercise. J. Natl. Cancer Inst. *107*. djv040–5. https://doi.org/10.1093/jnci/djv040.
10. Higgins, K.A., Park, D., Lee, G.Y., Curran, W.J., and Deng, X. (2014). Exercise-induced lung cancer regression: Mechanistic findings from a mouse model. Cancer *120*, 3302–3310. https://doi.org/10.1002/cncr.28878.
11. Moore, S.C., Lee, I.M., Weiderpass, E., Campbell, P.T., Sampson, J.N., Kitahara, C.M., Keadle, S.K., Arem, H., Berrington de Gonzalez, A., Hartge, P., et al. (2016). Association of leisure-time physical activity with risk of 26 types of cancer in 1.44 million adults. JAMA Intern. Med. *176*, 816–825. https://doi.org/10.1001/jamainternmed.2016.1548.
12. Being inactive and cancer risk - World Cancer Research Fund https://www.wcrf-uk.org/preventing-cancer/what-can-increase-your-risk-of-cancer/being-inactive-and-cancer-risk/.
13. Koelwyn, G.J., Jones, L.W., and Moslehi, J. (2014). Unravelling the causes of reduced peak oxygen consumption in patients with cancer: Complex, timely, and necessary. J. Am. Coll. Cardiol. *64*, 1320–1322. https://doi.org/10.1016/j.jacc.2014.07.949.
14. Cramer, L., Hildebrandt, B., Kung, T., Wichmann, K., Springer, J., Doehner, W., Sandek, A., Valentova, M., Stojakovic, T., Scharnagl, H., et al. (2014). Cardiovascular function and predictors of exercise capacity in patients with colorectal cancer. J. Am. Coll. Cardiol. *64*, 1310–1319. https://doi.org/10.1016/j.jacc.2014.07.948.
15. Jones, L.W., Courneya, K.S., Mackey, J.R., Muss, H.B., Pituskin, E.N., Scott, J.M., Hornsby, W.E., Coan, A.D., Herndon, J.E., Douglas, P.S., and Haykowsky, M. (2012). Cardiopulmonary function and age-related decline across the breast cancer: Survivorship continuum. J. Clin. Oncol. *30*, 2530–2537. https://doi.org/10.1200/JCO.2011.39.9014.
16. Piercy, K.L., Troiano, R.P., Ballard, R.M., Carlson, S.A., Fulton, J.E., Galuska, D.A., George, S.M., and Olson, R.D. (2018). The Physical Activity Guidelines for Americans. JAMA *320*, 2020–2028. https://doi.org/10.1001/JAMA.2018.14854.
17. Emery, A., Moore, S., Turner, J.E., and Campbell, J.P. (2022). Reframing How Physical Activity Reduces The Incidence of Clinically-Diagnosed Cancers: Appraising Exercise-Induced Immuno-Modulation As An Integral Mechanism. Front. Oncol. *12*, 788113. https://doi.org/10.3389/FONC.2022.788113.
18. Pedersen, L., Idorn, M., Olofsson, G.H., Lauenborg, B., Nookaew, I., Hansen, R.H., Johannesen, H.H., Becker, J.C., Pedersen, K.S., Dethlefsen, C., et al. (2016). Voluntary running suppresses tumor growth through epinephrine- and IL-6-dependent NK cell mobilization and redistribution. Cell Metabol. *23*, 554–562. https://doi.org/10.1016/j.cmet.2016.01.011.
19. Rundqvist, H., Velic, P., Barbieri, L., Gameiro, P.A., Bargiela, D., Gojkovic, M., Mijwel, S., Reitzner, S.M., and Johnson, R. (2020). Cytotoxic T-cells mediate exercise- induced reductions in tumor growth. Elife *9*, e59996.
20. Koelwyn, G.J., Zhuang, X., Tammela, T., Schietinger, A., and Jones, L.W. (2020). Exercise and immunometabolic regulation in cancer. Nat. Metab. *2*, 849–857. https://doi.org/10.1038/s42255-020-00277-4.
21. Campbell, J.P., and Turner, J.E. (2018). Debunking the myth of exercise-induced immune suppression: Redefining the impact of exercise on immunological health across the lifespan. Front. Immunol. *9*, 648. https://doi.org/10.3389/FIMMU.2018.00648/BIBTEX.
22. Gomes-Santos, I.L., Amoozgar, Z., Kumar, A.S., Ho, W.W., Roh, K., Talele, N.P., Curtis, H., Kawaguchi, K., Jain, R.K., and Fukumura, D. (2021). Exercise Training Improves Tumor Control by Increasing CD8+ T-cell Infiltration via CXCR3 Signaling and Sensitizes Breast Cancer to Immune Checkpoint Blockade. Cancer Immunol. Res. *9*, 765–778. https://doi.org/10.1158/2326-6066.CIR-20-0499.
23. Buck, M.D., O'Sullivan, D., Klein Geltink, R.I., Curtis, J.D., Chang, C.H., Sanin, D.E., Qiu, J., Kretz, O., Braas, D., van der Windt, G.J.W., et al. (2016). Mitochondrial Dynamics Controls T Cell Fate through Metabolic Programming. Cell *166*, 63–76. https://doi.org/10.1016/j.cell.2016.05.035.
24. Scharping, N.E., Menk, A.V., Moreci, R.S., Whetstone, R.D., Dadey, R.E., Watkins, S.C., Ferris, R.L., and Delgoffe, G.M. (2016). The Tumor Microenvironment Represses T Cell Mitochondrial Biogenesis to Drive Intratumoral T Cell Metabolic Insufficiency and Dysfunction. Immunity *45*, 374–388. https://doi.org/10.1016/j.immuni.2016.07.009.
25. Yu, Y.R., Imrichova, H., Wang, H., Chao, T., Xiao, Z., Gao, M., Rincon-Restrepo, M., Franco, F., Genolet, R., Cheng, W.C., et al. (2020). Disturbed mitochondrial dynamics in CD8+ TILs reinforce T cell exhaustion. Nat. Immunol. *21*, 1540–1551. https://doi.org/10.1038/s41590-020-0793-3.
26. Egan, B., and Zierath, J.R. (2013). Exercise metabolism and the molecular regulation of skeletal muscle adaptation. Cell Metabol. *17*, 162–184. https://doi.org/10.1016/j.cmet.2012.12.012.
27. Singer, M., Wang, C., Cong, L., Marjanovic, N.D., Kowalczyk, M.S., Zhang, H., Nyman, J., Sakuishi, K., Kurtulus, S., Gennert, D., et al. (2016). A Distinct Gene Module for Dysfunction Uncoupled from Activation in Tumor-Infiltrating T Cells. Cell *166*, 1500–1511.e9. https://doi.org/10.1016/j.cell.2016.08.052.
28. Sidarala, V., Zhu, J., Levi-D'Ancona, E., Pearson, G.L., Reck, E.C., Walker, E.M., Kaufman, B.A., and Soleimanpour, S.A. (2022). Mitofusin 1 and 2 regulation of mitochondrial DNA content is a critical determinant of glucose homeostasis. Nat. Commun. *13*, 2340. https://doi.org/10.1038/s41467-022-29945-7.
29. Zhang, J. (2013). Autophagy and mitophagy in cellular damage control. Redox Biol. *1*, 19–23. https://doi.org/10.1016/J.REDOX.2012.11.008.
30. Lee, S., Son, J.Y., Lee, J., and Cheong, H. (2023). Unraveling the Intricacies of Autophagy and Mitophagy: Implications in Cancer Biology. Cells *12*, 2742. https://doi.org/10.3390/CELLS12232742.
31. Liu, D., Wang, R., Grant, A.R., Zhang, J., Gordon, P.M., Wei, Y., and Chen, P. (2017). Immune adaptation to chronic intense exercise training: new microarray evidence. BMC Genom. *18*, 29. https://doi.org/10.1186/s12864-016-3388-5.
32. Schadler, K.L., Thomas, N.J., Galie, P.A., Bhang, D.H., Roby, K.C., Addai, P., Till, J.E., Sturgeon, K., Zaslavsky, A., Chen, C.S., and Ryeom, S. (2016). Tumor vessel normalization after aerobic exercise enhances chemotherapeutic efficacy. Oncotarget *7*, 65429–65440. https://doi.org/10.18632/oncotarget.11748.
33. Kruijsen-Jaarsma, M., Révész, D., Bierings, M.B., Buffart, L.M., and Takken, T. (2013). Effects of exercise on immune function in patients with cancer: A systematic review. Exerc. Immunol. Rev. *19*, 120–143.
34. Koelwyn, G.J., Quail, D.F., Zhang, X., White, R.M., and Jones, L.W. (2017). Exercise-dependent regulation of the tumour microenvironment. Nat. Rev. Cancer *17*, 620–632. https://doi.org/10.1038/nrc.2017.78.
35. Lakoski, S.G., Willis, B.L., Barlow, C.E., Leonard, D., Gao, A., Radford, N.B., Farrell, S.W., Douglas, P.S., Berry, J.D., Defina, L.F., and Jones, L.W. (2015). Midlife

cardiorespiratory fitness, incident cancer, and survival after cancer in men: The Cooper Center Longitudinal Study. JAMA Oncol. *1*, 231–237. https://doi.org/10.1001/jamaoncol.2015.0226.

36. Bonetto, A., Rupert, J.E., Barreto, R., and Zimmers, T.A. (2016). The Colon-26 Carcinoma Tumor-bearing Mouse as a Model for the Study of Cancer Cachexia. J. Vis. Exp. *30*, 54893. https://doi.org/10.3791/54893.
37. Bonetto, A., Kays, J.K., Parker, V.A., Matthews, R.R., Barreto, R., Puppa, M.J., Kang, K.S., Carson, J.A., Guise, T.A., Mohammad, K.S., et al. (2016). Differential bone loss in mouse models of colon cancer cachexia. Front. Physiol. *7*, 679. https://doi.org/10.3389/fphys.2016.00679.
38. Ballarò, R., Beltrà, M., De Lucia, S., Pin, F., Ranjbar, K., Hulmi, J.J., Costelli, P., and Penna, F. (2019). Moderate exercise in mice improves cancer plus chemotherapy-induced muscle wasting and mitochondrial alterations. Faseb. J. *33*, 5482–5494. https://doi.org/10.1096/FJ.201801862R.
39. Wenes, M., Shang, M., Di Matteo, M., Goveia, J., Martín-Pérez, R., Serneels, J., Prenen, H., Ghesquière, B., Carmeliet, P., and Mazzone, M. (2016). Macrophage Metabolism Controls Tumor Blood Vessel Morphogenesis and Metastasis. Cell Metabol. *24*, 701–715. https://doi.org/10.1016/j.cmet.2016.09.008.
40. Palazon, A., Tyrakis, P.A., Macias, D., Veliça, P., Rundqvist, H., Fitzpatrick, S., Vojnovic, N., Phan, A.T., Loman, N., Hedenfalk, I., et al. (2017). An HIF-1α/VEGF-A Axis in Cytotoxic T Cells Regulates Tumor Progression. Cancer Cell *32*, 669–683.e5. https://doi.org/10.1016/j.ccell.2017.10.003.
41. Repasky, E.A., Eng, J., and Hylander, B.L. (2015). Stress, metabolism and cancer: integrated pathways contributing to immune suppression. Cancer J. *21*, 97–103. https://doi.org/10.1097/PPO.0000000000000107.
42. Togashi, Y., Shitara, K., and Nishikawa, H. (2019). Regulatory T Cells in Cancer Immunosuppression — Implications for Anticancer Therapy. Nature reviews Clinical oncology *16*, 356–371. https://doi.org/10.1038/s41571-019-0175-7.
43. Desdín-Micó, G., Soto-Heredero, G., and Mittelbrunn, M. (2018). Mitochondrial Activity in T Cells. Mitochondrion *41*, 51–57. https://doi.org/10.1016/j.mito.2017.10.006.
44. Martínez-Reyes, I., and Chandel, N.S. (2020). Mitochondrial TCA cycle metabolites control physiology and disease. Nat. Commun. *11*, 102. https://doi.org/10.1038/s41467-019-13668-3.
45. Franco, F., Jaccard, A., Romero, P., Yu, Y.R., and Ho, P.C. (2020). Metabolic and epigenetic regulation of T-cell exhaustion. Nat. Metab. *2*, 1001–1012. https://doi.org/10.1038/s42255-020-00280-9.
46. Michalek, R.D., Gerriets, V.A., Jacobs, S.R., Macintyre, A.N., MacIver, N.J., Mason, E.F., Sullivan, S.A., Nichols, A.G., and Rathmell, J.C. (2011). Cutting Edge: Distinct Glycolytic and Lipid Oxidative Metabolic Programs Are Essential for Effector and Regulatory CD4 + T Cell Subsets. J. Immunol. *186*, 3299–3303. https://doi.org/10.4049/jimmunol.1003613.
47. Tan, H., Yang, K., Li, Y., Shaw, T.I., Wang, Y., Blanco, D.B., Wang, X., Cho, J.H., Wang, H., Rankin, S., et al. (2017). Integrative Proteomics and Phosphoproteomics Profiling Reveals Dynamic Signaling Networks and Bioenergetics Pathways Underlying T Cell Activation. Immunity *46*, 488–503. https://doi.org/10.1016/j.immuni.2017.02.010.
48. Diebold, L., and Chandel, N.S. (2016). Mitochondrial ROS regulation of proliferating cells. Free Radic. Biol. Med. *100*, 86–93. https://doi.org/10.1016/j.freeradbiomed.2016.04.198.
49. Dowling, R.J., Goodwin, P.J., and Stambolic, V. (2011). Understanding the benefit of metformin use in cancer treatment. BMC Med. *9*, 33–36. https://doi.org/10.1186/1741-7015-9-33/COMMENTS.
50. Yu, H., Zhong, X., Gao, P., Shi, J., Wu, Z., Guo, Z., Wang, Z., and Song, Y. (2019). The Potential Effect of Metformin on Cancer: An Umbrella Review. Front. Endocrinol. *10*, 617. https://doi.org/10.3389/FENDO.2019.00617.
51. Laker, R.C., Drake, J.C., Wilson, R.J., Lira, V.A., Lewellen, B.M., Ryall, K.A., Fisher, C.C., Zhang, M., Saucerman, J.J., Goodyear, L.J., et al. (2017). Ampk phosphorylation of Ulk1 is required for targeting of mitochondria to lysosomes in exercise-induced mitophagy. Nat. Commun. *8*, 548–613. https://doi.org/10.1038/s41467-017-00520-9.
52. Fan, W., and Evans, R.M. (2017). Exercise Mimetics: Impact on Health and Performance. Cell Metabol. *25*, 242–247. https://doi.org/10.1016/J.CMET.2016.10.022.
53. Gubert, C., and Hannan, A.J. (2021). Exercise mimetics: harnessing the therapeutic effects of physical activity. Nat. Rev. Drug Discov. *20*, 862–879. https://doi.org/10.1038/s41573-021-00217-1.
54. Huang, Q., Wu, M., Wu, X., Zhang, Y., and Xia, Y. (2022). Muscle-to-tumor crosstalk: The effect of exercise-induced myokine on cancer progression. Biochim. Biophys. Acta Rev. Canc *1877*, 188761. https://doi.org/10.1016/J.BBCAN.2022.188761.
55. Gebhardt, K., and Krüger, K. (2022). Supporting tumor therapy by exercise: boosting T cell immunity by myokines. Signal Transduct. Targeted Ther. *71*, 1–2. https://doi.org/10.1038/s41392-022-01116-6.
56. Hojman, P., Gehl, J., Christensen, J.F., and Pedersen, B.K. (2018). Molecular Mechanisms Linking Exercise to Cancer Prevention and Treatment. Cell Metabol. *27*, 10–21. https://doi.org/10.1016/j.cmet.2017.09.015.
57. Ferreira, J.C.B., Rolim, N.P.L., Bartholomeu, J.B., Gobatto, C.A., Kokubun, E., and Brum, P.C. (2007). Maximal lactate steady state in running mice: Effect of exercise training. Clin. Exp. Pharmacol. Physiol. *34*, 760–765. https://doi.org/10.1111/j.1440-1681.2007.04635.x.
58. Chang, C.H., Curtis, J.D., Maggi, L.B., Faubert, B., Villarino, A.V., O'Sullivan, D., Huang, S.C.C., Van Der Windt, G.J.W., Blagih, J., Qiu, J., et al. (2013). Posttranscriptional control of T cell effector function by aerobic glycolysis. Cell *153*, 1239–1251. https://doi.org/10.1016/j.cell.2013.05.016.
59. Subramanian, A., Tamayo, P., Mootha, V.K., Mukherjee, S., Ebert, B.L., Gillette, M.A., Paulovich, A., Pomeroy, S.L., Golub, T.R., Lander, E.S., and Mesirov, J.P. (2005). Gene set enrichment analysis: A knowledge-based approach for interpreting genome-wide expression profiles. Proc. Natl. Acad. Sci. USA *102*, 15545–15550. https://doi.org/10.1073/PNAS.0506580102/SUPPL_FILE/06580FIG7.JPG.

STAR★METHODS

KEY RESOURCES TABLE

REAGENT or RESOURCE	SOURCE	IDENTIFIER
Antibodies		
Total OXPHOS Rodent WB Antibody Cocktail	Abcam	Cat# ab110413; RRID:AB_2629281
Mouse monoclonal Pyruvate Dehydrogenase E1-alpha subunit [8D10E6]	Abcam	Cat# ab110334; RRID:AB_10866116
Mouse monoclonal Anti-Mitofusin 1 [11E91H12]	Abcam	Cat# ab126575, RRID:AB_11141234
IRDye® 800CW Goat anti-Mouse IgG Secondary Antibody	LI-COR Biosciences	Cat# 926-32210; RRID:AB_621842
Goat anti-Rat IgG (H + L) Cross-Adsorbed Secondary Antibody, Alexa Fluor™ 488	Thermo Fisher Scientific	Cat# A-11006; RRID:AB_2534074
Rat Anti-Mouse IFN-g (Interferon-gamma) Monoclonal Antibody, Unconjugated, Clone AN18	MABTECH	Cat# 3321-3-250; RRID:AB_907279
Fixable Viability Stain 575V	BD Biosciences	Cat# 565694; RRID:AB_2869702
TruStain FcX™ (anti-mouse CD16/32) Antibody	BioLegend	Cat# 101319; RRID:AB_1574975
Brilliant Violet 510™ anti-mouse CD45	BioLegend	Cat# 103138; RRID:AB_2561392
Armenian Hamster Anti-CD3e, PerCP-Cy5.5 Conjugated, Clone 145-2C11	BD Biosciences	Cat# 551163, RRID:AB_394082
Rat Anti-Mouse CD4, APC-H7 Conjugated, Clone GK1.5	BD Biosciences	Cat# 560181; RRID:AB_1645235
Rat Anti-CD8a, PE-Cy7 Conjugated, Clone 53-6.7	BD Biosciences	Cat# 552877; RRID:AB_394506
Anti-CD25 (PC61.5), eFluor™ 450, eBioscience	Thermo Fisher Scientific	Cat# 48-0251-82; RRID:AB_10671550
Rat Anti-Mouse Foxp3, PE Conjugated	BD Biosciences	Cat# 560414; RRID:AB_1645252
Brilliant Violet 421™ anti-mouse CD279 (PD-1)	BioLegend	Cat# 135221; RRID:AB_2561447
PE anti-mouse IFN-gamma	BioLegend	Cat# 505807; RRID:AB_315402
Chemicals, peptides, and recombinant proteins		
Collagenase, Type IV, powder	Thermo Fisher Scientific	Cat# 17104019
Deoxyribonuclease I from bovine pancreas	Sigma-Aldrich	Cat# D5025-15KU
Percoll density gradient media	Cytiva	Cat# 17089101
Tissue-Tek® O.C.T. Compound	Sakura Finetek	Cat# 4583
RPMI 1640 Medium	Gibco™	Cat# 11875093
Fetal Bovine Serum	Gibco™	Cat# A5256701
Penicillin-Streptomycin	Sigma-Aldrich	Cat# P4333
PBS, pH 7.4	Gibco™	Cat# 10010023
Phorbol 12-myristate 13-acetate	Sigma-Aldrich	Cat# P8139
Ionomycin calcium salt from Streptomyces conglobatus	Sigma-Aldrich	Cat# 56092-82-1
MitoTracker™ Green FM Dye, for flow cytometry	Thermo Fisher Scientific	Cat# M46750
TRIzol™ Reagent	Thermo Fisher Scientific	Cat# 15596018
ELISpot conjugate: Streptavidin-ALP	MABTECH	Cat# 3310-10-1000
Mounting Medium With DAPI - Aqueous, Fluoroshield	Abcam	Cat# ab104139

(*Continued on next page*)

Continued

REAGENT or RESOURCE	SOURCE	IDENTIFIER
Critical commercial assays		
High-Capacity cDNA Reverse Transcription Kit	Applied Biosystems™	Cat# 4368814
PowerUp SYBR Green Master Mix for qPCR	Applied Biosystems	Cat# A25776
Hypoxyprobe Kit	Hypoxyprobe, Inc	Cat# HP1-1000Kit
BD Cytofix/Cytoperm™ Plus Fixation/ Permeabilization Solution Kit with BD GolgiStop™	BD Biosciences	Cat# 554715
JC-1 Mitochondrial Membrane Potential Flow Cytometry Assay Kit	Cayman Chemical	Cat# 701560
AP Conjugate Substrate Kit	Bio-Rad	Cat# 1706432
Molecular Probes™ ATP Determination Kit	Thermo Fisher Scientific	Cat# A22066
EasySep™ Mouse CD8a Positive Selection Kit II	STEMCELL Technologies	Cat# 18953
BD Pharmingen™ Mouse Foxp3 Buffer Set	BD Biosciences	Cat# 560409
Deposited data		
Microarrays data	Liu D. et al.[31]	NCBI GEO: GSE68072
Datasets	Mendeley Data, Voltarelli, Vanessa (2024)	https://doi.org/10.17632/wb734hz2wc.1
Experimental models: Cell lines		
CT26.WT	ATCC®	CRL-2638; RRID:CVCL_7256
Experimental models: Organisms/strains		
Balb/c mice	ANILAB, Brazil	www.anilab.com.br
Oligonucleotides		
Primers for ATG5, ATG7, BNIP3, LC3B, HPRT1, PARK2, PINK1, ULK1, see Table S1	This paper	N/A
Software and algorithms		
GraphPad Prism 8	GraphPad Software	RRID:SCR_002798; http://www.graphpad.com/
FlowJo-V10	FlowJo Software	RRID:SCR_008520; https://www.flowjo.com/solutions/flowjo
ImageJ	NIH	RRID:SCR_003070; https://imagej.net/
StatSoft Statistica 7	StatSoft	RRID:SCR_014213; http://www.statsoft.com/Products/STATISTICA/Product-Index
BioRender	BioRender	RRID:SCR_018361; http://biorender.com

RESOURCE AVAILABILITY

Lead contact

Any additional information and requests for resources and reagents should be directed to and will be fulfilled by the lead contact, Vanessa A. Voltarelli (vvoltare@bidmc.harvard.edu).

Materials availability

This study did not generate new unique reagents.

Data and code availability

- This paper does not report original code.
- Data sets have been deposited at Mendeley. The DOI is listed in the key resources table. Microscopy data reported in this paper will be shared by the lead contact upon request.
- Any additional information required to reanalyze the data reported in this work is available from the lead contact upon request.

EXPERIMENTAL MODEL AND STUDY PARTICIPANT DETAILS

Animal model

Male Balb/c mice (8 weeks old) were housed in the animal facility of the School of Physical Education and Sport at University of Sao Paulo, in a temperature-controlled environment (22°C) and in a reversed 12:12-h dark-light cycle. Standard laboratory chow (Nuvital Nutrients, Curitiba, Brazil) and tap water were available *ad libitum*. The sample size for each experiment is indicated in the figures. Euthanasia was performed by cervical dislocation under isoflurane anesthesia (3.5%, administered in medical air enriched with oxygen). All procedures were in accordance with the Guide for the Care and Use of Laboratory Animals (National Institutes of Health, Bethesda, MD, USA) and with ethical principles in animal research adopted by the Brazilian Council for the Control of Animal Experimentation (CONCEA). In addition, this study was approved by the Ethical Committee of the School of Physical Education and Sport, University of Sao Paulo (protocol # 2017/02).

Running capacity test and aerobic exercise protocol

Aerobic exercise capacity was evaluated using a graded treadmill exercise test for mice previously standardized by our research group.[57] Mice were acclimatized to the treadmill for a week before the running capacity test (10 min of exercise/session in low speed). On the day of the test, each mouse was placed in individual treadmill lanes (Treadmill for Multiple Rodents, Grupo AVS – AVS Projetos, Sao Carlos, Brazil) and allowed to acclimatize for 5 min. After that, intensity of exercise was increased by 3 m/min (starting at 6 m/min) every 3 min until exhaustion. Exhaustion was defined as the moment when animals were unable to keep pace with the treadmill for up to 1 min. Mice were then randomized into sedentary and training groups based on the maximal velocity (Vmax) achieved in the incremental maximal test, ensuring that both groups exhibited similar average Vmax values with no significant statistical difference between them. Moderate-intensity aerobic exercise training (AET) sessions were performed at 60% of the mean Vmax, for 1 h/day, 5 days/week, for 30 days before tumor cells inoculation. Mice were kept under the same AET protocol for 9 or 13 days after tumor cells inoculation.

CT26 colon carcinoma cell line

CT26 cells were cultured in RPMI 1640 Medium supplemented with 10% Fetal Bovine Serum, 1X Penicillin-Streptomycin, at 37°C and 5% CO_2, and were regularly tested for Mycoplasma contamination. $1x10^6$ resuspended cells (in 100 μL of PBS) were inoculated subcutaneously in the upper flank 48 h after the last exercise session of the fourth week of AET. Evaluation of tumor growth was performed daily after tumor cell inoculation using a digital caliper. The largest and smallest tumor diameters were measured, and values obtained were used to calculate tumor volume using the following formula: V = 0.52 x (largest diameter) x (smallest diameter).[2]

METHOD DETAILS

Tumor histology

Solid tumors harvested 9 days after tumor cell inoculation were fixed in 4% paraformaldehyde (PFA) and embedded in paraffin for further staining with hematoxylin and eosin (H&E) using a standard protocol. H&E images were captured at 200× magnification. The number of tumor-infiltrating lymphocytes was evaluated using ImageJ's automatic particle counting tool. Five tumors per group were analyzed, with an average of 18 images per tumor. The quantitative data were expressed in number of particles/cells per area (μm^2).

For the assessment of tumor hypoxia, the Hypoxyprobe Kit was used. Animals received an intraperitoneal injection of pimonidazole HCl (60 mg/kg) 30 min before euthanasia. After harvesting, solid tumors were embedded in the cryoprotectant Tissue-Tek® O.C.T., frozen in dry ice, and stored at −80°C until sectioning. Upon thawing, tumor sections (5 μm) were fixed in cold acetone (4°C) for 10 min and incubated overnight at 4°C with anti-pimonidazole antibody (1:50, diluted in PBS containing 0.1% bovine serum albumin and 0.1% Tween 20). Subsequently, the sections were incubated for 1 h at room temperature with Alexa Fluor™ 488-conjugated secondary antibody (1:300). Slides were mounted using a mounting medium with DAPI for nucleus staining. Images were captured at 100× magnification. The area of tumor hypoxia was assessed by ImageJ (). Five tumors per group were analyzed, with an average of 10 images per tumor. The quantitative data were expressed in integrated density (fluorescence) corrected per area analyzed.

Tumor digestion

Tumors were cut into small pieces and further digested in 1X PBS containing 2% of Fetal Bovine Serum (FBS), collagenase type IV (2 mg/mL), and DNAse I (5U/mL), for 40 min at 37°C, with 150 rpm agitation. After digestion, the cell homogenate was filtered in 70 μm cell strainers and subjected to a Percoll gradient to obtain an enriched fraction of immune cells (total leukocytes). Inguinal draining lymph nodes (dLN) were mechanically homogenized in 70 μm cell strainers with 1X PBS supplemented with 2% of FBS to obtain an immune cells suspension.

Flow cytometry

Total immune cells isolated from digested tumors and dLN were first incubated with TruStain FcX™ antibody (1:100) for 10 min at 4°C to block nonspecific binding of immunoglobulin to the Fc receptors. Subsequently, the samples were incubated with fluorochrome-conjugated antibodies: FVS (Fixable Viability Stain Reagent), CD45, CD3, CD4, CD8, CD25, FOXP3, PD-1, and IFN-γ (1:40 dilution) for 30 min at 4°C. A list of the antibodies used can be found in the key resources table. Following staining, the samples were fixed with BD Fixation/Permeabilization Solution for 20 min at 4°C. Intracellular staining for FOXP3 was conducted after fixing and permeabilizing the cells using the BD Mouse Foxp3

Buffer Set. For the evaluation of IFN-γ production, a portion of the isolated cells was stimulated for 6 h in culture (37°C and 5% CO_2) with phorbol 12-myristate 13-acetate (PMA, 0.02 μg/mL) plus ionomycin (1 μg/mL), under Golgi blockade, before antibody incubation.[58] The cells were also stained with the fluorescent probes MitoTracker ™ Green FM and JC-1 for mitochondrial density and membrane potential assessment, respectively. Data were collected by the LSR Fortessa X-20 flow cytometer and analyzed using the FlowJo-V10 software.

ELISpot (Enzyme-Linked ImmunoSpot)

96-well PVDF membrane plates were activated for 30 s with 70% ethanol, washed three times with PBS, and incubated with an anti-IFN-γ antibody (7.5 μg/mL) for approximately 16 h. After incubation, wells were washed three times with PBS, blocked with 100 μL of media for 1 h, and 100,000 tumor-infiltrating immune cells were added in 100 μL of media. Cells were incubated for approximately 16 h at 37°C and 5% CO_2 while stimulated with PMA (0.02 μg/mL) and ionomycin (1 μg/mL). After incubation, plates were washed eight times with PBS (200 μL per well) and incubated for 3 h with an anti-IFN-γ antibody (1 μg/mL). Plates were washed eight times with PBS and wells incubated with Streptavidin-Alkaline Phosphatase (diluted 1:1000) for 1.5 h. Plates were washed eight times with PBS and a chromogen substrate (Alkaline phosphatase conjugate substrate kit) was added following manufacturer's instructions. The reaction was stopped after 45–60 min by washing the plate with tap water. The plate was left to dry for at least 24 h before counting spots on an AID classic ELISpot reader (AID software, Autoimmun Diagnostika GmbH (AID), Strassberg, Germany). Camera and counting settings were optimized and maintained for all samples. Data were expressed as spots per million cells.

ATP production in total leukocytes

The ATP production by total tumor-infiltrating immune cells was analyzed by bioluminescence using a commercial kit (Molecular Probes® ATP Determination Kit), and the assay was performed according to the manufacturer's instructions.

Immunoblotting

The protein expression of total tumor-infiltrating leukocytes was evaluated by Western Blotting. Initially, cells were mechanically disrupted in RIPA buffer, and further prepared in Laemmli sample buffer. Samples were separated by molecular weight on a SDS-PAGE gel, and proteins were then transferred to a nitrocellulose membrane. After blocking nonspecific antigenic sites, the membranes were incubated overnight at 4°C with primary antibodies for Total OXPHOS (1:500), PDH (Pyruvate Dehydrogenase E1-alpha subunit, 1:1000), and Mfn1 (Mitofusin 1, 1:1000). Secondary antibodies were incubated for 1 h at room temperature (IRDye 800 CW, LI-COR, 1:10,000). A list of the antibodies used can be found in the key resources table. Immunodetection was performed using the fluorescence method (Odyssey FC LI-COR, LI-COR Biosciences). Quantitative blot analyzes were performed using ImageJ.

Quantitative real-time PCR

Total RNA was extracted from frozen tumor samples using TRIzol® reagent, according to the manufacturer's instructions. Isolated RNA was quantified using a NanoDrop Spectrophotometer (NanoDrop Technologies, Rockland, DE) and denaturing agarose gel electrophoresis was used to assess the quality of the samples. A conventional reverse transcription reaction was performed to yield single-stranded cDNA. First strand cDNA was synthesized from 1μg of total RNA using the High-Capacity cDNA Reverse Transcription Kit according to the manufacturer's recommendations. The resulting cDNA was stored at −20°C until the expression analysis. The quantification of mRNA expression of genes was performed by RT-qPCR in a total volume of 10 μL, containing diluted cDNA template (1/10), forward and reverse primers (200 nM each - ATG5, ATG7, BNIP3, LC3B, PARK2, PINK1, and ULK1), and SYBR Green Master Mix. Primers sequences are described in Table S1. Gene expression was performed using the 7500 Real Time PCR System (Applied Biosystems), following the universal protocol of amplification: 95°C for 10 min, 40 cycles of 95°C for 15s, and 60°C for 1 min. Dissociation curves were performed to test primers specificity. Relative gene expression quantification was determined by $2^{-\Delta\Delta CT}$ method. Hprt1 was used as a reference gene.

Transmission Electron Microscopy (TEM)

$CD8^+$ T cells were first purified from tumors using the EasySep™ Mouse CD8a Positive Selection Kit II according to the manufacturer's instructions. After that, the purified $CD8^+$ TILs (an average of $5x10^3$ cells per sample) were pelleted and fixed in 3.0% glutaraldehyde in 0.1M cacodylate buffer for 2 h at 4°C. The pellets were then rinsed in buffer, post-fixed in 1.0% osmium tetroxide (OsO_4), and counterstained with aqueous 1% uranyl acetate. The samples dehydration was performed in graded ethanol incubations, and then they were embedded in standard Spurr resin. The resin embedded tissues were polymerized at 58°C for 72 h. Ultrathin sections were placed on grids, stained with lead citrate, and images were collected using a transmission electron microscope TECNAI FEI G20 - 200 Kv. Mitochondrial number, area, perimeter, and elongation were quantified by ImageJ (Scion Corporation, NIH, USA). Four samples/mice per group were analyzed, in which an average of ten $CD8^+$ TILs were identified (50 to 120 mitochondria analyzed per sample).

In-silico analysis of a microarray dataset

The enrichment plot for oxidative phosphorylation-related genes was performed using the Gene Set Enrichment Analysis (GSEA),[59] comparing a previously published microarray data from peripheral blood leukocytes in young endurance athletes versus healthy controls (GEO database, Series GSE68072).[31]

QUANTIFICATION AND STATISTICAL ANALYSIS

Statistical analysis

Data are presented as mean ± standard error. Data normality was assessed through Shapiro-Wilk's test. Comparisons for two groups were calculated using the unpaired Student's *t* test. For more than two groups, comparisons were made by one-way ANOVA, followed by Duncan's post hoc. Repeated measures data were analyzed by repeated measures ANOVA or by fitting a mixed effects model. The software StatSoft Statistica 7 was used for the analysis. The value of $p < 0.05$ was used to determine statistical differences between groups.